




Analytical WKB theory for high-harmonic generation and its application to massive Dirac electronsHidetoshi Taya ^{1,2,*} Masaru Hongo ^{3,1,†} and Tatsuhiko N. Ikeda ^{4,‡}¹*RIKEN iTHEMS, RIKEN, Wako 351-0198, Japan*²*Research and Education Center for Natural Sciences, Keio University 4-1-1 Hiyoshi, Kohoku-ku, Yokohama, Kanagawa 223-8521, Japan*³*Department of Physics, University of Illinois, Chicago, Illinois 60607, USA*⁴*Institute for Solid State Physics, University of Tokyo, Kashiwa, Chiba 277-8581, Japan*

(Received 1 June 2021; revised 7 October 2021; accepted 11 October 2021; published 21 October 2021)

We propose an analytical approach to high-harmonic generation (HHG) for nonperturbative low-frequency and high-intensity fields based on the (Jeffreys-)Wentzel-Kramers-Brillouin (WKB) approximation. By properly taking into account Stokes phenomena of WKB solutions, we obtain wave functions that systematically include the repetitive dynamics of production and acceleration of electron-hole pairs and quantum interference due to phase accumulation between different pair production times (Stückelberg phase). Using the obtained wave functions without relying on any phenomenological assumptions, we explicitly compute electric current (including intra- and interband contributions) as the source of HHG for a massive Dirac system in (1+1) dimensions under an ac electric field. We demonstrate that the WKB approximation agrees well with numerical results obtained by solving the time-dependent Schrödinger equation and point out that the quantum interference is important in HHG. We also predict in the deep nonperturbative regime that (1) harmonic intensities oscillate with respect to electric-field amplitude E_0 and frequency Ω , with a period determined by the Stückelberg phase, (2) the cutoff order of HHG is determined by $2eE_0/\hbar\Omega^2$, with e being the electron charge, and that (3) noninteger harmonics, controlled by the Stückelberg phase, appear as a transient effect. Our WKB theory is particularly suited for a parameter regime, where the Keldysh parameter $\gamma = (\Delta/2)\Omega/eE_0$, with Δ being the gap size, is small. This parameter regime corresponds to intense lasers in the terahertz regime for realistic massive Dirac materials. Our analysis implies that the so-called HHG plateau can be observed at the terahertz frequency within the current technology.

DOI: [10.1103/PhysRevB.104.L140305](https://doi.org/10.1103/PhysRevB.104.L140305)

Introduction. High-harmonic generation (HHG) is one of the most intriguing phenomena in nonlinear optics [1]. Owing to developments in laser technologies over the decades, HHG has been observed and analyzed in various media (e.g., atomic gases [2–4], liquids [5,6], semiconductors [7–11], graphene [12–15], superconductors [16–19], strongly correlated electrons [20–23], and amorphous solids [24,25]), providing a unique opportunity to explore the fully nonperturbative regime of matter-field interactions and rich applications such as attosecond light sources and ultrafast imaging methods [26]. HHG has also been predicted in the fundamental theory of quantum electrodynamics (QED), i.e., the QED vacuum emits high harmonics when exposed to strong fields exceeding the Schwinger limit [27,28].

One of the greatest theoretical challenges to elucidate the HHG mechanism is to understand nonperturbative electron dynamics under low-frequency and high-intensity fields [29,30]. Typically, theorists numerically solve the time-dependent Schrödinger equation (TDSE) [31–33] (or von Neumann equation [34–37]) to simulate electric current and/or polarization as the source of HHG. These studies have provided numerical evidence that the interplay

between the intra- and interband electron dynamics plays an essential role. Meanwhile, analytical methods are demanded to deepen the fundamental understanding and to analyze numerically inaccessible parameter regimes such as the low-frequency limit. Analytical theories exist for the simplest single-band model [7,38], which, however, completely neglects the interband dynamics. For multiband models, there are Floquet-theoretical approaches [39,40], but analytical results have been limited to the high-frequency regime where the laser frequency Ω exceeds the band gap Δ . Thus, an analytical HHG theory has not been established for the quintessential low-frequency and high-intensity fields.

In this Letter, we present an analytical method to study HHG in the nonperturbative low-frequency and high-intensity regime. Our method is based on the (Jeffreys-)Wentzel-Kramers-Brillouin [(J)WKB [41–44]] approximation, which has been extended by mathematicians since the 1980s (leading to the exact WKB analysis) [45–52] and applied successfully to various physical problems such as tunneling pair production [53–57] and nonlinear radiative processes under strong fields [58–60]. The WKB approximation is a semiclassical method valid in the formal limit $\hbar \rightarrow 0$ or equivalently when the Keldysh parameter [55,61–64]

$$\gamma \equiv \frac{\Omega(\Delta/2)}{eE_0} \quad (1)$$

*hidetoshi.taya@riken.jp

†masaru.hongo@riken.jp

‡tikeda@issp.u-tokyo.ac.jp

is sufficiently small (e and E_0 are the electron charge and electric-field amplitude, respectively, and we assume $eE_0 > 0$ and set the speed of light to be unity). Hence, it is suited for low-frequency and high-intensity fields, where nonperturbative processes, such as quantum tunneling (Landau-Zener transition [65–68] or Sauter-Schwinger effect [69–71]), take place. Another advantage is that one can explicitly solve TDSE (up to some order of \hbar) and can compute observables directly from the wave function without any *ad hoc* assumptions. The wave function has microscopic information on the nonperturbative electron-hole dynamics under strong fields, which enables us to understand the HHG mechanism.

Setup. For concreteness, we consider massive Dirac electrons in (1+1) dimensions under a time-dependent electric field $E(t)$. The Hamiltonian reads

$$H \equiv \begin{pmatrix} \Delta/2 & k - eA \\ k - eA & -\Delta/2 \end{pmatrix}, \quad (2)$$

where $A(t) \equiv -\int^t dt' E(t')$ is the vector potential, k is canonical momentum (or Bloch momentum in solids), and Δ is the gap energy. Note that the Hamiltonian (2) is relativistic and linear in k , so that the diamagnetic term A^2 is absent unlike nonrelativistic Hamiltonians. The following argument also applies to general two-level systems, e.g., Dirac materials (including QED) in other dimensions [72], topological insulators [73], semiconductors [29], and graphene [74,75]. We assume that the electric field is turned on at $t = t_{\text{in}}$, before which the system is in the ground state, and compute the induced electric current as the source of HHG. As we will clarify soon, our WKB theory is valid in the nonperturbative regime $\gamma \lesssim 1$. For realistic massive Dirac materials $\Delta = O(10 \text{ meV})$ [76,77], this corresponds to intense ($E_0 \gtrsim 1 \text{ kV/cm}$) terahertz [$\Omega/(2\pi) \sim 10^{12} \text{ Hz}$] lasers, which are available within the current laser technology used in the terahertz HHG observations [15,78,79].

WKB solution and Stokes phenomenon. To solve TDSE with the Hamiltonian (2), we expand the solution ψ by WKB wave functions ψ_{\pm} ,

$$\psi(t) = \alpha \psi_{-}(t) + \beta \psi_{+}(t), \quad (3)$$

where α and β are called Stokes constants and satisfy $1 = |\alpha|^2 + |\beta|^2$ so that $1 = \psi^{\dagger} \psi$. We work within the lowest-order WKB approximation, where ψ_{\pm} is given by the instantaneous eigenstates for the Hamiltonian (2) with dynamical phase factors,

$$\begin{aligned} \psi_{+} &= \frac{1}{\sqrt{2}} \sqrt{1 - \frac{\Delta/2}{\epsilon}} \begin{pmatrix} +\frac{k-eA}{\epsilon - \Delta/2} \\ 1 \end{pmatrix} e^{-\frac{i}{\hbar} \int_0^t dt' \epsilon}, \\ \psi_{-} &= \frac{1}{\sqrt{2}} \sqrt{1 - \frac{\Delta/2}{\epsilon}} \begin{pmatrix} 1 \\ -\frac{k-eA}{\epsilon - \Delta/2} \end{pmatrix} e^{+\frac{i}{\hbar} \int_0^t dt' \epsilon}, \end{aligned} \quad (4)$$

with $\epsilon \equiv \sqrt{(\Delta/2)^2 + (k - eA)^2}$ being the instantaneous eigenenergy, which includes the intraband acceleration by the external field.

To determine the Stokes constants α and β , we analytically continue the instantaneous energy onto the complex z plane ($\epsilon(t \in \mathbb{R}) \rightarrow \epsilon(z \in \mathbb{C})$) and analyze the associated Stokes graph (see Fig. 1). The Stokes constants α and β take

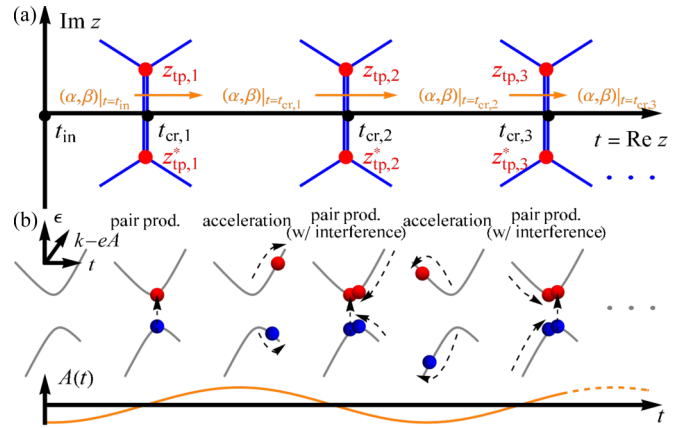


FIG. 1. (a) A typical Stokes graph, composed of Stokes lines (blue lines) and turning points (red points), and (b) the corresponding physical processes during the real-time evolution.

constant values within each Stokes region, which is defined as a region in the complex z plane separated by Stokes lines $\mathcal{C}_{z^{\text{tp}}} \equiv \{z \in \mathbb{C} \mid 0 = \text{Im}[\frac{i}{\hbar} \int_{z^{\text{tp}}}^z dz \epsilon]\}$, with $z^{\text{tp}} \in \mathbb{C}$ being turning points such that $0 \equiv \epsilon(z^{\text{tp}})$. For the instantaneous energy ϵ that are real on the real axis, turning points and Stokes lines are symmetric in the upper and lower complex z planes, and the pairs of turning points ($z^{\text{tp}}, z^{\text{tp}*}$) are connected with a doubly degenerate Stokes line crossing the real axis only once at $t^{\text{cr}} = \{t \in \mathbb{R} \mid 0 = \text{Im}[\frac{i}{\hbar} \int_{z^{\text{tp}}}^t dz \epsilon]\}$ [55]. Whenever $t \in \mathbb{R}$ crosses a degenerate Stokes line at $t = t^{\text{cr}}$ during the time evolution, the Stokes constants α and β jump discontinuously (Stokes phenomenon) as [55,80]

$$\begin{pmatrix} \alpha \\ \beta \end{pmatrix} \Big|_{t_n^{\text{cr}+0^+} = \begin{pmatrix} 1 & (-1)^n e^{-\frac{\sigma_n}{\hbar}} \\ -(-1)^n e^{-\frac{\sigma_n}{\hbar}} & 1 \end{pmatrix} \begin{pmatrix} \alpha \\ \beta \end{pmatrix} \Big|_{t_n^{\text{cr}-0^+}, \quad (5)$$

where $\sigma_n \equiv 2i \int_0^{z_n^{\text{tp}}} dz \epsilon$ ($\text{Re } \sigma_n > 0$), t_n^{cr} ($t_{\text{in}} < t_1^{\text{cr}} < t_2^{\text{cr}} < \dots$) is the n th crossing associated with ($z_n^{\text{tp}}, z_n^{\text{tp}*}$), and we neglected subleading $O(e^{-\frac{2}{\hbar} \text{Re } \sigma_n})$ terms by assuming $\hbar \rightarrow 0$. Using Eq. (5), we find an approximate solution, starting from the initial ground-state wave function $(\alpha, \beta)|_{t=t_{\text{in}}} = (1, 0)$, as

$$\psi = \psi_{-} - \sum_n (-1)^n e^{-\frac{\sigma_n}{\hbar}} \Theta(t - t_n^{\text{cr}}) \psi_{+}. \quad (6)$$

The Stokes constant β (5) [i.e., the coefficient in front of ψ_{+} in Eq. (6)] gives the probability amplitude from the initial ground state to an excited state with the instantaneous basis (4). Thus, $\beta \neq 0$ means that electron-hole pair production occurs (see Fig. 1), and $|\beta|^2$ gives the pair production number. The typical magnitude of the production number is determined by the exponential factor $e^{-\frac{1}{\hbar} \text{Re } \sigma_n}$. Note that Eq. (6) takes the form of superposition of the wave functions describing the pair production at different times. The phase factor $e^{-\frac{i}{\hbar} \text{Im } \sigma_n}$, related to the so-called Stückelberg phase, is thus responsible for quantum interference effect [67,80–82]: When pair production occurs repetitively, the Stückelberg

phase, i.e., the relative phase between each wave function,

$$\theta_{n,n'} \equiv \frac{2}{\hbar} \int_{t_n^{\text{cr}}}^{t_{n'}^{\text{cr}}} dt \epsilon = -\frac{1}{\hbar} (\text{Im} \sigma_n - \text{Im} \sigma_{n'}) \neq 0, \quad (7)$$

gives rise to destructive and constructive interferences, which suppress and enhance the production, respectively. Note that our Stokes constants α and β (5) neglect pair annihilation processes followed after the production, which are higher-order effects $O(e^{-\frac{2}{\hbar} \text{Re} \sigma_n})$.

Within the lowest-order WKB approximation (4), the production number $|\beta|^2$ shows stepwise time dependence, meaning that each production process is treated as an instantaneous one that occurs exactly at $t = t_n^{\text{cr}}$. In reality, the stepwise evolution is an approximation, and pair production takes finite time $\delta t \neq 0$. Under an electric field, for a pair production to occur via quantum tunneling, an electron in the valence band needs to tunnel a distance $\sim \Delta/eE_0$ to the conduction band, and hence $\delta t \sim \gamma \Omega^{-1}$ with the Keldysh parameter γ . Thus, the WKB approximation would not work for very high harmonics $N \equiv \omega/\Omega \gtrsim (2\pi/\delta t)/\Omega \sim 2\pi\gamma^{-1}$ or when $\gamma \gtrsim 2\pi/N$. This also implies that the WKB approximation cannot describe perturbative excitation processes, which dominate for large γ [55,61–64].

WKB result for electric current. We compute the electric current $J \equiv \langle -\delta H/\delta A \rangle = e\psi^\dagger \sigma^1 \psi$ at each momentum k . The WKB approximation (6) gives J as a sum of the valence-, intra-, and interband contributions, $J = J_{\text{val}} + J_{\text{intra}} + J_{\text{inter}}$, where

$$\begin{aligned} J_{\text{val}} &\equiv e\psi_-^\dagger \sigma^1 \psi_- = -ev, \\ J_{\text{intra}} &\equiv \sum_{\pm} |\beta|^2 (\pm e) \psi_{\pm}^\dagger \sigma^1 \psi_{\pm} \\ &= 2ev \left| \sum_n (-1)^n e^{-\frac{\sigma_n}{\hbar}} \Theta(t - t_n^{\text{cr}}) \right|^2, \\ J_{\text{inter}} &\equiv 2e \text{Re}(\alpha\beta^* \psi_+^\dagger \sigma^1 \psi_-) \\ &= e \frac{\Delta}{\epsilon} \sum_n (-1)^n e^{-\frac{1}{\hbar} \text{Re} \sigma_n} \Theta(t - t_n^{\text{cr}}) \cos \left(\frac{2}{\hbar} \int_{t_n^{\text{cr}}}^t dt \epsilon \right), \end{aligned} \quad (8)$$

with velocity $v \equiv (k - eA)/\epsilon$. Being proportional to v , J_{val} (J_{intra}) is accompanied by valence-band electrons (electron-hole pairs) accelerated along the band(s). J_{inter} originates from interference between conduction- and valence-band electrons (or dipole [83]), as is evident from the wave-function overlap $\text{Re}(\alpha\beta^* \psi_+^\dagger \sigma^1 \psi_-)$. Since the actual observable is the difference from the ground state, we subtract J_{val} and focus on

$$J_{\text{obs}} \equiv J - J_{\text{val}} = J_{\text{intra}} + J_{\text{inter}}. \quad (9)$$

This is a standard subtraction scheme widely used in quantum-field theory in external fields [84]. Also, in the condensed-matter context, the subtracted J_{val} amounts to be when summed over the entire Brillouin zone. Note that the observable currents J_{intra} and J_{inter} reproduce the phenomenological expressions used in previous studies on semiconductor HHG [36,37].

According to Eq. (8), the nonlinear response to the applied field arises not only from the pair production factor $e^{-\frac{\sigma_n}{\hbar}}$ but

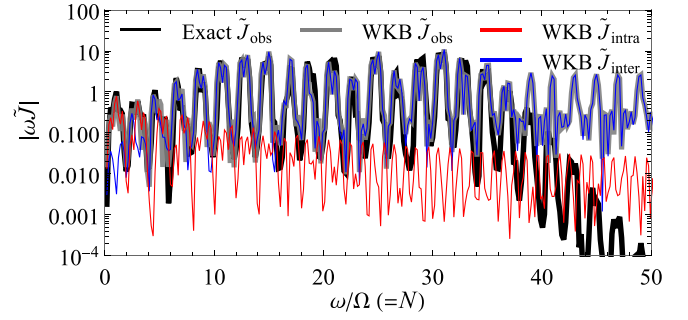


FIG. 2. HHG spectrum for the oscillating field (10), with $\Omega/(\Delta/2) = 1/4$, $eE_0/(\Delta/2)^2 = 1$ (i.e., $\gamma = 1/4$), and $\Omega t_{\text{in}} = -17\pi/3$, $T_w = 2|t_{\text{in}}|$. The parameter set corresponds to, e.g., $\Omega/2\pi = 1$ THz and $E_0 = 4.2$ kV/cm for a Dirac material with Fermi velocity $v_F = 10^6$ m/s and mass $\Delta = 33$ meV.

also from the velocity v in J_{intra} . Whereas the nonlinearity of v is absent for the quadratic dispersion, it can be significant for the linear one in massless Dirac systems [78,79,85]. The strong nonlinearity survives to some extent even in our massive case.

HHG by ac electric field. As a demonstration, we consider a monochromatic ac field,

$$eA = -\frac{eE_0}{\Omega} \sin(\Omega t), \quad (10)$$

and take $k \rightarrow 0$, as pair production at large k may be energetically disfavored (see Ref. [86] for situations where various k 's become important). For the field (10), the wave function encounters two crossings in a cycle $t_n^{\text{cr}} \in \frac{\pi}{\Omega} \mathbb{Z}$, i.e., pairs are produced twice in a cycle. This is similar to the three-step process in the gas HHG [3,4]. Although our WKB approach also applies to other k 's, their analytical expressions become more complex. We leave for future work this generalization and summing the results over k 's. In exchange for restricting ourselves to $k \rightarrow 0$, we will obtain analytical closed formulas, which would at least qualitatively capture the HHG in the massive Dirac electrons.

We compute the Fourier spectrum of the observable $\tilde{J}_{\text{obs}} \equiv \int_{-\infty}^{+\infty} dt e^{i\omega t} W J_{\text{obs}} = \tilde{J}_{\text{intra}} + \tilde{J}_{\text{inter}}$, where we insert a window function W with width T_w to avoid contaminations due to the finiteness of fields/measurements [31,87]. Here, we chose the Hann window $W \equiv \Theta(t - t_{\text{in}})\Theta(T_w + t_{\text{in}} - t) \sin^2[\pi(t - t_{\text{in}})/T_w]$ and confirmed that the results are insensitive to the choice of W . One can obtain a closed analytical expression for J_{obs} under Eq. (10), from which one can compute the spectrum \tilde{J}_{obs} numerically or even analytically under certain approximations [88].

The HHG spectrum obtained from the WKB approximation (8) agrees well for small γ with the exact one obtained by numerically solving TDSE; see Fig. 2. Due to the limitation of the WKB approximation, the discrepancy for very high harmonics appears at $N \gtrsim 35$ in Fig. 2, which is consistent with our estimate $\sim 2\pi\gamma^{-1}$.

Our WKB result confirms that the interband contribution dominates over the intraband one, except for the low harmonics ($N \lesssim 3$ in Fig. 2) [36,37]. This means that the interband contribution is the origin of the plateau structure in the HHG

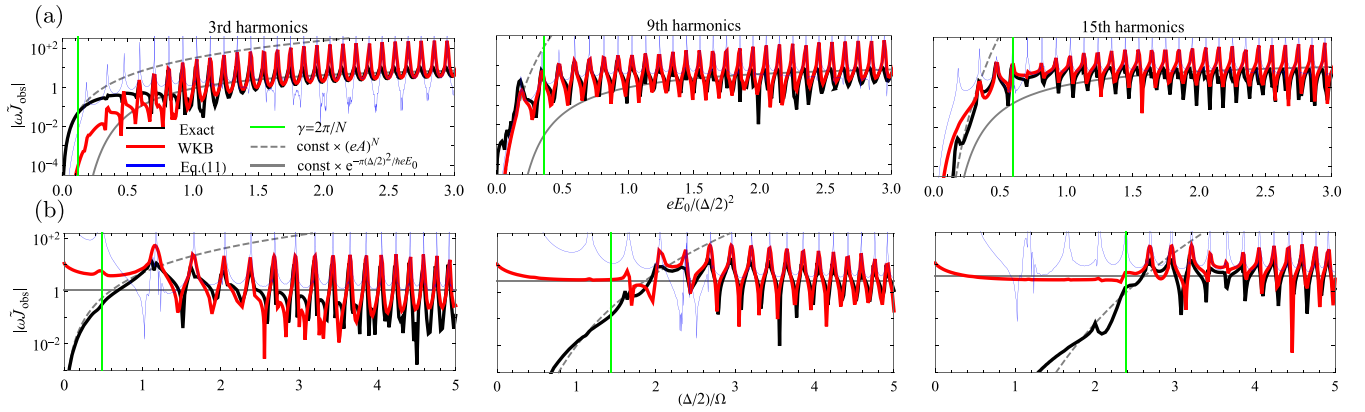


FIG. 3. The magnitude of $N = 3$ (left), 9 (middle), and 15 (right) harmonic peaks plotted against amplitude eE_0 with fixed frequency $\Omega/(\Delta/2) = 1/4$ (a) and inverse frequency Ω^{-1} with fixed amplitude $eE_0/(\Delta/2)^2 = 1$ (b). The other parameters are chosen as $\Omega t_{\text{in}} = -17\pi/3$, $T_w = 2|t_{\text{in}}|$.

spectrum [8]. One may estimate the location of the cutoff by using the saddle-point method [4,36,37] when evaluating the Fourier integral of the WKB expressions (8). The stationary conditions for the intra- and interband currents are given by $\omega = 0$ and $2\epsilon - \hbar|\omega| = 0$, respectively. The former condition confirms why the intraband current contributes only to the low harmonics. The latter condition can have real solutions when $\Delta/\hbar\Omega \lesssim N \lesssim \sqrt{\Delta^2 + 4(|k| + eE_0/\Omega)^2/\hbar\Omega} \sim 2(|k| + eE_0/\Omega)/\hbar\Omega$. If the stationary points are imaginary, the saddle-point action acquires a positive real part and then the spectrum \tilde{J}_{inter} is suppressed exponentially. Therefore, it is sufficient to pick up the contribution from the real solution only, which yields that the upper cutoff of the HHG spectra for $k \rightarrow 0$ is given by

$$N_{\text{cut}} \sim \frac{2eE_0}{\hbar\Omega^2} \quad (11)$$

(~ 32 in Fig. 2). The linear dependence on E_0 is consistent with semiconductor experiments [7], and the frequency dependence Ω^{-2} is our prediction in the massive Dirac electrons, which is worth testing in experiments (see Ref. [39] for a similar prediction in a charge-density-wave material). Note that the lower cutoff $N \sim \Delta/\hbar\Omega$ (~ 8 in Fig. 2) for the interband current is also consistent with Fig. 2.

To further investigate the HHG spectrum, we plot the eE_0 and Ω^{-1} dependence of each harmonic intensity in Fig. 3. The WKB result reproduces the exact one in the nonperturbative high-intensity and low-frequency regime $\gamma \lesssim 2\pi/N$, while it fails for the perturbative low-intensity and high-frequency one $\gamma \gtrsim 2\pi/N$. In the perturbative regime, the N th harmonic intensity shows a power dependence on the potential $(eA)^N \propto (eE_0/\Omega)^N$. This indicates that a perturbative N -photon process dominates, which cannot be captured by the WKB approximation. On the other hand, the harmonic intensities saturate (with

oscillations) in the nonperturbative regime. The typical magnitude of the currents asymptote $|\tilde{J}_{\text{intra}}| \rightarrow |\beta|^2 \propto e^{-\pi \frac{(\Delta/2)^2}{eE_0}}$ and $|\tilde{J}_{\text{inter}}| \rightarrow |\beta| \propto e^{-\pi \frac{(\Delta/2)^2}{2eE_0}}$, which are independent of Ω and N . This explains why the harmonic intensities have a weak N dependence in the nonperturbative regime and the plateau appears in Fig. 2. Notice that the nonperturbative dependence on eE_0 is the manifestation that the production is driven by tunneling and agrees with the tunneling production formula [65–71].

The oscillating behavior in Fig. 3 is caused by the quantum interference. When the interference becomes destructive (constructive), the production and associated HHG are suppressed (enhanced). For our field (10) with the limit $k \rightarrow 0$, the Stückelberg phase can be decomposed as $\theta_{n,n'} = (n - n')\theta$, where $\theta \equiv \frac{2}{\hbar} \int_{t_{\text{in}}^{\text{cr}}}^{t_{\text{in}}^{\text{cr}+1}} dt \epsilon = \frac{2}{\hbar} \int_0^{\pi/\Omega} dt \epsilon$ is the phase for two successive production and is independent of n . Then, Eq. (5) indicates that the most destructive (constructive) interference occurs when θ matches even- (odd-) integer multiples of π . As shown analytically below, θ is roughly proportional to eE_0/Ω^2 , and hence the harmonic intensities oscillate with eE_0 and Ω . This Stückelberg-phase mechanism for the oscillation is analogous to that in the gas HHG [89,90] and would also apply to the recent semiconductor HHG experiment [91]. Note that we focus on $k \rightarrow 0$ although the physically observed currents are obtained in principle by collecting contributions from different k 's over the Brillouin zone. Since the Stückelberg phase depends smoothly on k , the sum over k would smoothen the oscillating behavior in Fig. 3. As noted above, we leave it for future work to extend our analytical WKB theory for different k 's.

Analytical formula in the low-frequency limit. To get deeper insights, we analytically carry out the Fourier integration for the WKB result in the limit of $\gamma, k \rightarrow 0$ [88],

$$\tilde{J}_{\text{intra}} \sim e^{-\frac{2\text{Re}\sigma}{\hbar}} \frac{-i}{\pi \cos^2 \frac{\theta}{2}} \sum_{n=-\infty}^{\infty} \left[\sum_{\pm} e^{+i\pi \left(\lceil \frac{t_{\text{in}}}{\pi/\Omega} \rceil - \frac{1}{2} \right) (\mp \frac{\theta}{\pi} - 1)} \frac{\sin \frac{\theta}{2}}{4(n - \frac{\theta}{2\pi})} \tilde{W} \left(\omega - \Omega \mp 2 \left(n - \frac{\theta}{2\pi} \right) \Omega \right) - \frac{\tilde{W}(\omega - (2n - 1)\Omega)}{2n - 1} \right],$$

$$\tilde{J}_{\text{inter}} \sim e^{-\frac{\text{Re}\sigma}{\hbar}} \frac{-i(-1)^{\lceil \frac{t_{\text{in}}}{\pi/\Omega} \rceil} \gamma}{4\pi \cos \frac{\theta}{2}} \sum_{n=-\infty}^{+\infty} \sum_{\pm} \left[(\ln \gamma^2 + 2H_{\pm n - 1/2}) e^{+i\pi \left(\lceil \frac{t_{\text{in}}}{\pi/\Omega} \rceil - \frac{1}{2} \right) (\mp \frac{\theta}{\pi} - 1)} \tilde{W} \left(\omega \mp 2 \left(n - \frac{\theta}{2\pi} \right) \Omega \right) \right]$$

$$+\left(\ln(4\gamma^2) - \left((-1)^n \cos \frac{\theta}{2} - 1\right) H_{\frac{n}{2} \pm \frac{\theta}{4\pi} - 1} + \left((-1)^n \cos \frac{\theta}{2} + 1\right) H_{\frac{n}{2} \pm \frac{\theta}{4\pi} - \frac{1}{2}}\right) \tilde{W}(\omega - (2n - 1)\Omega), \quad (12)$$

where \tilde{W} is the Fourier transform of the window function (i.e., a regularized delta function), H_n is the harmonic number, $\text{Re } \sigma = \pi \frac{(\Delta/2)^2}{eE_0} [1 + O(\gamma^2)]$, and $\theta = \frac{4eE_0}{\hbar\Omega^2} [1 + O(\gamma^2)]$.

The analytic formula (12) captures the important features of the exact numerical results for small γ ; see Fig. 3. The saturation behavior is determined by the overall factor $e^{-\frac{\text{Re}\sigma}{\hbar}}$, reflecting the abundance of pair production due to tunneling. The oscillating behavior derives from $\cos \frac{\theta}{2}$ in the denominators. Whenever θ hits an odd-integer multiple of π , each harmonic intensity is maximized, as anticipated from the quantum-interference argument. Incidentally, the second terms in the square brackets give odd-order harmonics, while the first ones give noninteger split peaks around the integer harmonics with $\delta N = \pm\theta/\pi$. This splitting is a transient effect, as is evident from the t_{in} dependence, and is tunable by changing the Stückelberg phase θ , which can be varied, e.g., with the carrier-envelope phase [92].

Summary. We have studied HHG in a massive Dirac system based on the lowest-order WKB approximation, including Stokes phenomena. We have shown that the WKB approximation provides a powerful analytical framework to study HHG in the nonperturbative low-frequency and high-intensity regime and well reproduces the exact results of TDSE. Our

results imply that the repetitive dynamics of production and acceleration of electron-hole pairs and quantum interference due to the Stückelberg phase are the essence of HHG. We have also predicted some characteristic features of HHG in the deep nonperturbative regime, such as the scaling of the cutoff $N_{\text{cut}} \propto eE_0/\Omega^2$, the oscillation of harmonic intensities with a period determined by the Stückelberg phase $\theta \propto eE_0/\Omega^2$, and the noninteger splittings of harmonic peaks $\delta N \propto \theta$ as a transient effect. Our WKB approach applies to various media such as Dirac/Weyl materials (including QED), topological insulators, semiconductors, and graphene, paving the way toward a universal understanding of HHG beyond gases.

Acknowledgments. The authors thank the Yukawa Institute for Theoretical Physics at Kyoto University, where this work was initiated during YITP-T-20-05 The Schwinger Effect and Strong-Field Physics Workshop, and are supported by Non-Equilibrium Working group (NEW) at RIKEN Interdisciplinary Theoretical and Mathematical Sciences Program (iTHEMS). H.T. thanks Antonino Di Piazza for useful discussions. M.H. was supported by the U.S. Department of Energy, Office of Science, Office of Nuclear Physics under Award No. DE-FG0201ER41195. T.N.I. was supported by JSPS KAKENHI Grants No. JP18K13495 and No. JP21K13852.

- [1] T. Brabec and F. Krausz, Intense few-cycle laser fields: Frontiers of nonlinear optics, *Rev. Mod. Phys.* **72**, 545 (2000).
- [2] M. Ferray, A. L'Huillier, X. F. Li, L. A. Lompre, G. Mainfray, and C. Manus, Multiple-harmonic conversion of 1064 nm radiation in rare gases, *J. Phys. B: At. Mol. Opt. Phys.* **21**, L31 (1988).
- [3] P. B. Corkum, Plasma Perspective on Strong Field Multiphoton Ionization, *Phys. Rev. Lett.* **71**, 1994 (1993).
- [4] M. Lewenstein, P. Balcou, M. Y. Ivanov, A. L'Huillier, and P. B. Corkum, Theory of high-harmonic generation by low-frequency laser fields, *Phys. Rev. A* **49**, 2117 (1994).
- [5] P. Heissler, E. Lugovoy, R. Hörlein, L. Waldecker, J. Wenz, M. Heigoldt, K. Khrennikov, S. Karsch, F. Krausz, B. Abel, and G. D. Tsakiris, Using the third state of matter: High harmonic generation from liquid targets, *New J. Phys.* **16**, 113045 (2014).
- [6] T. T. Luu, Z. Yin, A. Jain, T. Gaumnitz, Y. Pertot, J. Ma, and H. J. Wörner, Extreme-ultraviolet high-harmonic generation in liquids, *Nat. Commun.* **9**, 3723 (2018).
- [7] S. Ghimire, A. D. DiChiara, E. Sistrunk, P. Agostini, L. F. DiMauro, and D. A. Reis, Observation of high-order harmonic generation in a bulk crystal, *Nat. Phys.* **7**, 138 (2011).
- [8] O. Schubert, M. Hohenleutner, F. Langer, B. Urbanek, C. Lange, U. Huttner, D. Golde, T. Meier, M. Kira, S. W. Koch *et al.*, Sub-cycle control of terahertz high-harmonic generation by dynamical Bloch oscillations, *Nat. Photonics* **8**, 119 (2014).
- [9] M. Hohenleutner, F. Langer, O. Schubert, M. Knorr, U. Huttner, S. W. Koch, M. Kira, and R. Huber, Real-time observation of interfering crystal electrons in high-harmonic generation, *Nature (London)* **523**, 572 (2015).
- [10] T. T. Luu, M. Garg, S. Y. Kruchinin, A. Moulet, M. T. Hassan, and E. Goulielmakis, Extreme ultraviolet high-harmonic spectroscopy of solids, *Nature (London)* **521**, 498 (2015).
- [11] K. Kaneshima, Y. Shinohara, K. Takeuchi, N. Ishii, K. Imasaka, T. Kaji, S. Ashihara, K. L. Ishikawa, and J. Itatani, Polarization-Resolved Study of High Harmonics from Bulk Semiconductors, *Phys. Rev. Lett.* **120**, 243903 (2018).
- [12] S. A. Mikhailov and K. Ziegler, Nonlinear electromagnetic response of graphene: Frequency multiplication and the self-consistent-field effects, *J. Phys.: Condens. Matter* **20**, 384204 (2008).
- [13] I. Al-Naib, J. E. Sipe, and M. M. Dignam, High harmonic generation in undoped graphene: Interplay of inter- and intraband dynamics, *Phys. Rev. B* **90**, 245423 (2014).
- [14] N. Yoshikawa, T. Tamaya, and K. Tanaka, High-harmonic generation in graphene enhanced by elliptically polarized light excitation, *Science* **356**, 736 (2017).
- [15] H. A. Hafez, S. Kovalev, J.-C. Deinert, Z. Mics, B. Green, N. Awari, M. Chen, S. Germanskiy, U. Lehnert, J. Teichert, Z. Wang, K.-J. Tielrooij, Z. Liu, Z. Chen, A. Narita, K. Müllen, M. Bonn, M. Gensch, and D. Turchinovich, Extremely efficient terahertz high-harmonic generation in graphene by hot Dirac fermions, *Nature (London)* **561**, 507 (2018).
- [16] R. Matsunaga, N. Tsuji, H. Fujita, A. Sugioka, K. Makise, Y. Uzawa, H. Terai, Z. Wang, H. Aoki, and R. Shimano, Light-induced collective pseudospin precession resonating with Higgs mode in a superconductor, *Science* **345**, 1145 (2014).
- [17] Y. Kawakami, T. Amano, Y. Yoneyama, Y. Akamine, H. Itoh, G. Kawaguchi, H. M. Yamamoto, H. Kishida, K. Itoh, T. Sasaki,

- S. Ishihara, Y. Tanaka, K. Yonemitsu, and S. Iwai, Nonlinear charge oscillation driven by a single-cycle light field in an organic superconductor, *Nat. Photonics* **12**, 474 (2018).
- [18] K. Yonemitsu, Charge oscillations emerging after application of an intense light field to superconductors on a dimer lattice, *J. Phys. Soc. Jpn.* **87**, 124703 (2018).
- [19] S. Nakamura, K. Katsumi, H. Terai, and R. Shimano, Nonreciprocal Terahertz Second-Harmonic Generation in Superconducting NbN under Supercurrent Injection, *Phys. Rev. Lett.* **125**, 097004 (2020).
- [20] Y. Murakami, M. Eckstein, and P. Werner, High-Harmonic Generation in Mott Insulators, *Phys. Rev. Lett.* **121**, 057405 (2018).
- [21] S. Imai, A. Ono, and S. Ishihara, High Harmonic Generation in a Correlated Electron System, *Phys. Rev. Lett.* **124**, 157404 (2020).
- [22] M. Lysne, Y. Murakami, and P. Werner, Signatures of bosonic excitations in high-harmonic spectra of Mott insulators, *Phys. Rev. B* **101**, 195139 (2020).
- [23] A. Roy, S. Bera, and K. Saha, Nonlinear dynamical response of interacting bosons to synthetic electric field, *Phys. Rev. Research* **2**, 043133 (2020).
- [24] Y. S. You, Y. Yin, Y. Wu, A. Chew, X. Ren, F. Zhuang, S. Gholam-Mirzaei, M. Chini, Z. Chang, and S. Ghimire, High-harmonic generation in amorphous solids, *Nat. Commun.* **8**, 724 (2017).
- [25] P. Jürgens, B. Liewehr, B. Kruse, C. Peltz, D. Engel, A. Husakou, T. Witting, M. Ivanov, M. Vrakking, T. Fennel *et al.*, Origin of strong-field-induced low-order harmonic generation in amorphous quartz, *Nat. Phys.* **16**, 1035 (2020).
- [26] G. Vampa, T. J. Hammond, N. Thiré, B. E. Schmidt, F. Légaré, C. R. McDonald, T. Brabec, D. D. Klug, and P. B. Corkum, All-Optical Reconstruction of Crystal Band Structure, *Phys. Rev. Lett.* **115**, 193603 (2015).
- [27] A. Di Piazza, K. Z. Hatsagortsyan, and C. H. Keitel, Harmonic generation from laser-driven vacuum, *Phys. Rev. D* **72**, 085005 (2005).
- [28] A. Fedotov and N. Narozhny, Generation of harmonics by a focused laser beam in the vacuum, *Phys. Lett. A* **362**, 1 (2007).
- [29] U. Huttner, M. Kira, and S. W. Koch, Ultrahigh off-resonant field effects in semiconductors, *Laser Photonics Rev.* **11**, 1700049 (2017).
- [30] S. Ghimire and D. A. Reis, High-harmonic generation from solids, *Nat. Phys.* **15**, 10 (2019).
- [31] M. Wu, S. Ghimire, D. A. Reis, K. J. Schafer, and M. B. Gaarde, High-harmonic generation from Bloch electrons in solids, *Phys. Rev. A* **91**, 043839 (2015).
- [32] T. Ikemachi, Y. Shinohara, T. Sato, J. Yumoto, M. Kuwata-Gonokami, and K. L. Ishikawa, Trajectory analysis of high-order-harmonic generation from periodic crystals, *Phys. Rev. A* **95**, 043416 (2017).
- [33] E. N. Osika, A. Chacón, L. Ortmann, N. Suárez, J. A. Pérez-Hernández, B. Szafran, M. F. Ciappina, F. Sols, A. S. Landsman, and M. Lewenstein, Wannier-Bloch Approach to Localization in High-Harmonics Generation in Solids, *Phys. Rev. X* **7**, 021017 (2017).
- [34] D. Golde, T. Meier, and S. W. Koch, High harmonics generated in semiconductor nanostructures by the coupled dynamics of optical inter- and intraband excitations, *Phys. Rev. B* **77**, 075330 (2008).
- [35] D. Golde, M. Kira, T. Meier, and S. W. Koch, Microscopic theory of the extremely nonlinear terahertz response of semiconductors, *Phys. Status Solidi B* **248**, 863 (2011).
- [36] G. Vampa, C. R. McDonald, G. Orlando, D. D. Klug, P. B. Corkum, and T. Brabec, Theoretical Analysis of High-Harmonic Generation in Solids, *Phys. Rev. Lett.* **113**, 073901 (2014).
- [37] G. Vampa, C. R. McDonald, G. Orlando, P. B. Corkum, and T. Brabec, Semiclassical analysis of high harmonic generation in bulk crystals, *Phys. Rev. B* **91**, 064302 (2015).
- [38] K. A. Pronin, A. D. Bandrauk, and A. A. Ovchinnikov, Harmonic generation by a one-dimensional conductor: Exact results, *Phys. Rev. B* **50**, 3473 (1994).
- [39] T. N. Ikeda, K. Chinzei, and H. Tsunetsugu, Floquet-theoretical formulation and analysis of high-order harmonic generation in solids, *Phys. Rev. A* **98**, 063426 (2018).
- [40] K. Chinzei and T. N. Ikeda, Disorder effects on the origin of high-order harmonic generation in solids, *Phys. Rev. Research* **2**, 013033 (2020).
- [41] G. Wentzel, Eine Verallgemeinerung der Quantenbedingungen für die Zwecke der Wellenmechanik, *Z. Phys.* **38**, 518 (1926).
- [42] H. Kramers, Wellenmechanik und halbzahlige Quantisierung, *Z. Phys.* **39**, 828 (1926).
- [43] L. Brillouin, La mécanique ondulatoire de Schrödinger; une méthode générale de résolution par approximations successives, *C. R. Hebd. Seances Acad. Sci.* **183**, 24 (1926).
- [44] H. Jeffreys, On certain approximate solutions of linear differential equations of the second order, *Proc. London Math. Soc.* **s2-23**, 428 (1924).
- [45] A. Voros, The return of the quartic oscillator. The complex WKB method, *Ann. I.H.P.: Phys. Theor.* **39**, 211 (1983).
- [46] B. Candelpergher, J. C. Nosmas, and F. Pham, Approche de la résurgence, *Actualités mathématiques* (Hermann, Paris, 1993) (in French).
- [47] H. Dillinger, E. Delabaere, and F. Pham, Résurgence de Voros et périodes des courbes hyperelliptiques, *Ann. Inst. Fourier* **43**, 163 (1993).
- [48] E. Delabaere, H. Dillinger, and F. Pham, Exact semiclassical expansions for one-dimensional quantum oscillators, *J. Math. Phys.* **38**, 6126 (1997).
- [49] E. Delabaere and F. Pham, Resurgent methods in semi-classical asymptotics, *Ann. I.H.P.: Phys. Theor.* **71**, 1 (1999).
- [50] T. Aoki, T. Kawai, and Y. Takei, The Bender-Wu analysis and the Voros theory, in *ICM-90 Satellite Conference Proceedings*, edited by M. Kashiwara and T. Miwa (Springer, Tokyo, 1991).
- [51] T. Aoki, T. Kawai, and Y. Takei, The Bender-Wu analysis and the Voros theory II, in *Algebraic Analysis and Around: In Honor of Professor Masaki Kashiwara's 60th Birthday*, edited by T. Miwa, A. Matsuo, T. Nakashima, and Y. Saito, *Advanced Studies in Pure Mathematics Vol. 54* (World Scientific, Singapore, 2009), p. 19.
- [52] T. Aoki, T. Kawai, and Y. Takei, Algebraic analysis of singular perturbations: On exact WKB analysis, Report No. RIMS-947, 1993 (unpublished).
- [53] S. Enomoto and T. Matsuda, The exact WKB for cosmological particle production, *J. High Energy Phys.* **03** (2021) 090.
- [54] S. Enomoto and T. Matsuda, The exact WKB and the Landau-Zener transition for asymmetry in cosmological particle production, [arXiv:2104.02312](https://arxiv.org/abs/2104.02312).

- [55] H. Taya, T. Fujimori, T. Misumi, M. Nitta, and N. Sakai, Exact WKB analysis of the vacuum pair production by time-dependent electric fields, *J. High Energy Phys.* **03** (2021) 82.
- [56] S. Hashiba and Y. Yamada, Stokes phenomenon and gravitational particle production—How to evaluate it in practice, *J. Cosmol. Astropart. Phys.* **2021**, 022 (2021).
- [57] C. M. Sou, X. Tong, and Y. Wang, Chemical-potential-assisted particle production in FRW spacetimes, *J. High Energy Phys.* **06** (2021) 129.
- [58] E. Raicher, S. Eliezer, C. H. Keitel, and K. Z. Hatsagortsyan, Semiclassical limitations for photon emission in strong external fields, *Phys. Rev. A* **99**, 052513 (2019).
- [59] A. Di Piazza, Ultrarelativistic Electron States in a General Background Electromagnetic Field, *Phys. Rev. Lett.* **113**, 040402 (2014).
- [60] A. Di Piazza, WKB electron wave functions in a tightly focused laser beam, *Phys. Rev. D* **103**, 076011 (2021).
- [61] L. V. Keldysh, Ionization in the field of a strong electromagnetic wave, *J. Exp. Theor. Phys.* **20**, 1307 (1965).
- [62] E. Brezin and C. Itzykson, Pair production in vacuum by an alternating field, *Phys. Rev. D* **2**, 1191 (1970).
- [63] V. S. Popov, Production of e^+e^- pairs in an alternating external field, *JETP Lett.* **13**, 185 (1971).
- [64] H. Taya, H. Fujii, and K. Itakura, Finite pulse effects on e^+e^- pair creation from strong electric fields, *Phys. Rev. D* **90**, 014039 (2014).
- [65] L. D. Landau, Zur theorie der phasenumwandlungen II, *Phys. Z. Sowjetunion* **11**, 26 (1937).
- [66] C. Zener, Non-adiabatic crossing of energy levels, *Proc. R. Soc. London, Ser. A* **137**, 696 (1932).
- [67] E. K. G. Stückelberg, *Theorie der unelastischen Stöße zwischen Atomen* (Birkhäuser, Basel, 1933).
- [68] E. Majorana, Atomi orientati in campo magnetico variabile, *Nuovo Cimento* **9**, 43 (1932).
- [69] F. Sauter, Über das Verhalten eines Elektrons im homogenen elektrischen Feld nach der relativistischen Theorie Diracs, *Z. Phys.* **69**, 742 (1931).
- [70] W. Heisenberg and H. Euler, Consequences of Dirac's theory of positrons, *Z. Phys.* **98**, 714 (1936).
- [71] J. S. Schwinger, On gauge invariance and vacuum polarization, *Phys. Rev.* **82**, 664 (1951).
- [72] When an applied electric field is spatially uniform and linearly polarized, spin degrees of freedom are degenerated regardless of the spacetime dimension and hence the Dirac Hamiltonian reduces in general to a two-level system, describing the valence- and conduction-band electron degrees of freedom.
- [73] C. Jürß and D. Bauer, High-harmonic generation in Su-Schrieffer-Heeger chains, *Phys. Rev. B* **99**, 195428 (2019).
- [74] E. McCann and V. I. Fal'ko, Landau-Level Degeneracy and Quantum Hall Effect in a Graphite Bilayer, *Phys. Rev. Lett.* **96**, 086805 (2006).
- [75] E. McCann and M. Koshino, The electronic properties of bilayer graphene, *Rep. Prog. Phys.* **76**, 056503 (2013).
- [76] Y. L. Chen, J.-H. Chu, J. G. Analytis, Z. K. Liu, K. Igarashi, H.-H. Kuo, X. L. Qi, S. K. Mo, R. G. Moore, D. H. Lu, M. Hashimoto, T. Sasagawa, S. C. Zhang, I. R. Fisher, Z. Hussain, and Z. X. Shen, Massive Dirac fermion on the surface of a magnetically doped topological insulator, *Science* **329**, 659 (2010).
- [77] H.-Z. Lu, W.-Y. Shan, W. Yao, Q. Niu, and S.-Q. Shen, Massive Dirac fermions and spin physics in an ultrathin film of topological insulator, *Phys. Rev. B* **81**, 115407 (2010).
- [78] B. Cheng, N. Kanda, T. N. Ikeda, T. Matsuda, P. Xia, T. Schumann, S. Stemmer, J. Itatani, N. P. Armitage, and R. Matsunaga, Efficient Terahertz Harmonic Generation with Coherent Acceleration of Electrons in the Dirac Semimetal Cd_3As_2 , *Phys. Rev. Lett.* **124**, 117402 (2020).
- [79] S. Kovalev, R. M. A. Dantas, S. Germanskiy, J.-C. Deinert, B. Green, I. Ilyakov, N. Awari, M. Chen, M. Bawatna, J. Ling, F. Xiu, P. H. M. van Loosdrecht, P. Surowka, T. Oka, and Z. Wang, Non-perturbative terahertz high-harmonic generation in the three-dimensional Dirac semimetal Cd_3As_2 , *Nat. Commun.* **11**, 2451 (2020).
- [80] C. K. Dumlu and G. V. Dunne, Interference effects in schwinger vacuum pair production for time-dependent laser pulses, *Phys. Rev. D* **83**, 065028 (2011).
- [81] C. K. Dumlu and G. V. Dunne, The Stokes Phenomenon and Schwinger Vacuum Pair Production in Time-Dependent Laser Pulses, *Phys. Rev. Lett.* **104**, 250402 (2010).
- [82] S. Shevchenko, S. Ashhab, and F. Nori, Landau-Zener-Stückelberg interferometry, *Phys. Rep.* **492**, 1 (2010).
- [83] N. Tanji, Dynamical view of pair creation in uniform electric and magnetic fields, *Ann. Phys.* **324**, 1691 (2009).
- [84] N. D. Birrell and P. C. W. Davies, *Quantum Fields in Curved Space*, Cambridge Monographs on Mathematical Physics (Cambridge University Press, Cambridge, UK, 1984).
- [85] S. A. Mikhailov, Non-linear electromagnetic response of graphene, *Europhys. Lett.* **79**, 27002 (2007).
- [86] L. Yue and M. B. Gaarde, Expanded view of electron-hole recollisions in solid-state high-order harmonic generation: Full-Brillouin-zone tunneling and imperfect recollisions, *Phys. Rev. A* **103**, 063105 (2021).
- [87] T. N. Ikeda, High-order nonlinear optical response of a twisted bilayer graphene, *Phys. Rev. Research* **2**, 032015(R) (2020).
- [88] See Supplemental Material at <http://link.aps.org/supplemental/10.1103/PhysRevB.104.L140305> for details of the computation of the Fourier spectrum \tilde{J}_{obs} for the oscillating electric field $eA = -(eE_0/\Omega) \sin(\Omega t)$ with $k = 0$.
- [89] E. S. Toma, P. Antoine, A. De Bohan, and H. G. Müller, Resonance-enhanced high-harmonic generation, *J. Phys. B: At. Mol. Opt. Phys.* **32**, 5843 (1999).
- [90] S. V. Popruzhenko, P. A. Korneev, S. P. Goreslavski, and W. Becker, Laser-Induced Recollision Phenomena: Interference Resonances at Channel Closings, *Phys. Rev. Lett.* **89**, 023001 (2002).
- [91] P. Xia, T. Tamaya, C. Kim, F. Lu, T. Kanai, N. Ishii, J. Itatani, H. Akiyama, and T. Kato, High-harmonic generation in GaAs beyond the perturbative regime, *Phys. Rev. B* **104**, L121202 (2021).
- [92] C. P. Schmid, L. Weigl, P. Grössing, V. Junk, C. Gorini, S. Schlauderer, S. Ito, M. Meierhofer, N. Hofmann, D. Afanasiev, J. Crewse, K. A. Kokh, O. E. Tereshchenko, J. Gädde, F. Evers, J. Wilhelm, K. Richter, U. Höfer, and R. Huber, Tunable non-integer high-harmonic generation in a topological insulator, *Nature (London)* **593**, 385 (2021).